JGR Atmospheres

RESEARCH ARTICLE
10.1029/2022JD037708

Compound Events in South America Using the CORDEX-CORE Ensemble: Current Climate Conditions and Future Projections in a Global Warming Scenario

M. E. Olmo[1,2,3,4], T. Weber[1], C. Teichmann[1], and M. L. Bettolli[2,3,4]

[1]Climate Service Center Germany (GERICS), Helmholtz-Zentrum Hereon, Hamburg, Germany, [2]Department of Atmospheric and Ocean Sciences, Faculty of Exact and Natural Sciences, University of Buenos Aires (DCAO-FCEN-UBA), Buenos Aires, Argentina, [3]National Council of Scientific and Technical Research (CONICET), Buenos Aires, Argentina, [4]Institut Franco-Argentin d'Estudes sur le Climat et Ses Impacts (IFAECI IRL 3351/CNRS-IRD-CONICET-UBA), Buenos Aires, Argentina

Abstract Climate hazards associated with compound events (CEs) have lately received increasing attention over South America (SA) due to their potential risks and amplification of impacts. This work addressed the evaluation of different temperature- and precipitation-based CE in SA considering the CORDEX-CORE ensemble of regional climate models (RCMs) and their driving earth system models (ESMs) in the reference period 1981–2010 and the late 21st century (2070–2099), for the Representative Concentration Pathways (RCPs) 2.6 and 8.5 scenarios. The assessment focused on model performance for the individual events—heatwaves (HWs), Extreme rainfall (ER) days, and dry-spells (DSs)—and their compound occurrence in terms of climatological frequency and duration. The spatial patterns of individual events were adequately reproduced by the RCMs, evidencing general overestimations in extreme precipitation intensities. In terms of CE, the frequencies of coincident HWs and DSs (sequential DSs and ER) were remarkable over central-eastern Brazil and southern SA (southeastern SA). The main features of CE were generally well-simulated by the RCMs, although they presented regional differences such as an underestimation of the maximum frequencies of these two CE in northeastern Brazil and southeastern SA, respectively. The high-resolution information was generally in line with the larger-scale driving ESMs. The climate change signal analysis generally showed robust future increases in CE frequency and duration in different areas of SA, as for coincident HWs and DSs (sequential DSs and ER) over northern SA and southern Brazil (southeastern SA). This was mostly consistent among the RCMs ensemble and notably strengthened in the worst-case scenario (RCP 8.5).

Key Points:

- Coincident heatwaves and dry-spells (DSs) and sequential DSs and extreme rainfall are remarkable compound events (CEs) over South America
- Regional climate models can reproduce the frequency and duration of CEs, but with some regional differences
- CEs are generally expected to be more frequent in the late 21st century, particularly in the Representative Concentration Pathway 8.5 scenario

Supporting Information:

Supporting Information may be found in the online version of this article.

Correspondence to:

M. E. Olmo,
Matias.Olmo@hereon.de

Citation:

Olmo, M. E., Weber, T., Teichmann, C., & Bettolli, M. L. (2022). Compound events in South America using the CORDEX-CORE ensemble: Current climate conditions and future projections in a global warming scenario. *Journal of Geophysical Research: Atmospheres*, *127*, e2022JD037708. https://doi.org/10.1029/2022JD037708

Received 21 AUG 2022
Accepted 20 OCT 2022

Author Contributions:

Conceptualization: M. E. Olmo, T. Weber, C. Teichmann, M. L. Bettolli
Investigation: M. E. Olmo, T. Weber, C. Teichmann, M. L. Bettolli
Methodology: M. E. Olmo, T. Weber, C. Teichmann, M. L. Bettolli
Resources: T. Weber, C. Teichmann
Software: T. Weber
Supervision: T. Weber, C. Teichmann, M. L. Bettolli
Visualization: M. E. Olmo
Writing – original draft: M. E. Olmo, M. L. Bettolli

1. Introduction

Arising recognition has lately been seen on climate extremes that occur close together in space or time, since the combination of drivers and hazards contributes to societal or environmental risk. In this context, the *Intergovernmental Panel on Climate Change* (IPCC) defines a compound event (CE) when two or more extreme events occur simultaneously or successively, when different extreme events combined imply an amplification of the impacts, or when individual events that are not extreme by themselves can lead to an extreme event or impact when they occur together, inducing an emerging risk (IPCC, 2012). Thereby, the scientific community sustains that a better understanding of CE provides the basis for assessing potential high impact events in future projections and can improve the inter-communication between the different disciplines and decision makers (Bevacqua et al., 2021; Zscheischler et al., 2018).

Temperature and precipitation compound extremes have been widely analyzed in different scales and regions around the world, such as record-breaking warm and dry seasons or the joint occurrence of heavy precipitation and extreme temperatures, using both observations and model outputs (Hao et al., 2018; Orth et al., 2021; Ridder et al., 2021; Tencer et al., 2014; Vogel et al., 2020; Wu et al., 2021). Many socio-environmental impacts are associated with extremely hot and dry conditions, such as increasing tree mortality and insect outbreaks, heat stress, spread of diseases, fire enhancement and crop failure, whereas social inequality contributes to the increasing risk (Brouillet & Joussaume, 2019; Orth et al., 2021; Silva et al., 2020). Focused over Africa, Weber et al. (2020) assessed the influence of multiple CE on population exposure in a climate change scenario, highlighting that the projected increasing exposure was mainly driven by the interaction between these climate hazards—such as

compound heatwaves (HWs) and droughts—and population growth. Thus, this kind of evaluation is critical for climate-related policy making.

Lately, the occurrence of CE over South America (SA) has received increasing attention. SA is a continent with important emerging economies, rainfed agricultural activities, expanding populations and urban centers. A rising trend in flood-associated damage and documented effects of HWs on mortality stand out over SA (Almeira et al., 2016; IPCC, 2021; Marengo et al., 2022; Vörösmarty et al., 2013). Recent episodes of intense HWs during anomalous dry conditions over central SA were associated with specific hazards, such as wildfire risk and water insecurity, that affected human activities and natural systems (Marengo et al., 2021). Previous works pointed out the occurrence of diverse compound extremes across the different regions of SA. At the daily scale, extreme temperatures notably enhance the likelihood of heavy precipitation events over southern SA, exhibiting upward trends in the recent period, particularly during the austral warm season. These events were associated with specific large-scale atmospheric circulation patterns that determine their occurrence in sectorized areas of southern SA, including the influence of El Niño (Gulizia & Pirotte, 2021; Olmo et al., 2020; Tencer et al., 2016). Moreover, robust increases on dry and warm compound extremes were detected over northern SA, affected by the occurrence of this oscillation (Hao et al., 2018; Zscheischler et al., 2017). This is expected to intensify based on future projections of different climate models (Coppola et al., 2021; Wu et al., 2021).

Earth system models (ESMs) have been designed to describe large-scale climate characteristics and the potential evolution of climate under future emission scenarios (Moss et al., 2010). However, ESMs still show major deficiencies when it comes to representing specific processes that may condition the regional climate. For instance, they have limitations in simulating certain physical processes such as frontal or convective systems, which may result in uncertainties in capturing the observed dependence between precipitation and temperature and further lead to some discrepancies when assessing the evaluation of CEs (Hao et al., 2018). In this sense, regional climate models (RCMs) produce high-resolution climate information needed to assess impact and decision-making policies. They can capture regional scale forcings that ESMs cannot reproduce, such as land-sea contrast and topography (Ambrizzi et al., 2018; Di Luca et al., 2016). This is particularly valuable over SA, where the main climatic features are strongly influenced by the presence of the Andes Mountain range, which extends longitudinally over the continent and is related to the contrasting climate over its eastern and western sides. The Andes mountains act as a topographic barrier for the zonal flow, favor the meridional exchange of air masses and alter the initiation and maintenance of convective systems (Espinoza et al., 2020; Rasmussen & Houze, 2016).

RCMs have demonstrated skills in reproducing the main features of individual temperature and precipitation extremes over SA (Carril et al., 2016; Dereczynski et al., 2020; López-Franca et al., 2016; Olmo & Bettolli, 2021; Reboita et al., 2021; Solman et al., 2019). Tencer et al. (2016) has examined over La Plata basin—the second basin of SA in terms of river discharge and size—the RCMs potential for simulating compound temperature and precipitation extreme events, displaying good skills in representing the temperature-precipitation dependance, although the spatial pattern was not adequately captured. More recently, based on the framework given by the *Coordinated Regional Climate Downscaling Experiment* (CORDEX), a growing number of RCMs simulations with increasing temporal and spatial resolution is available over SA, therefore motivating the analysis of compound extremes over the continent using RCMs. In relation to this, Coppola et al. (2021) identified some regions of SA as hotspots for increasing compound HWs and extreme precipitation events in the future using RCMs and ESMs.

Hence, the potential for critical economic damage and loss of lives motivates a deeper understanding of these climate hazards and their future changes in a context of global warming. In this context, we make use of the high-resolution RCMs from the recent project embedded in the CORDEX framework, the *Coordinated Output for Regional Evaluation* (CORE) (Giorgi et al., 2022; Gutowski et al., 2016). Thereby, the aim of this work is to evaluate the representation of different compound climate extreme events over SA by a set of CORDEX-CORE RCMs, considering their historical period and future projections under different climate change scenarios.

2. Data and Methods

2.1. Reference Data Set and Climate Model Simulations

CEs were calculated during the reference period 1981–2010 considering daily maximum temperature and daily precipitation data (Tx and Pr, respectively) from the ERA5 reanalysis at a spatial resolution of 0.25° (~28 km) as reference ERA5 is the fifth-generation reanalysis produced by the *European Center for*

Table 1
Regional Climate Models (RCMs) and Their Driving Earth System Models (ESMs) Used in This Study

RCM (label)	RCM acronym	CMIP5 ESM	ESM resolution	Reference
RegCM4v7	RegCM	HadGEM2-ES	1.9° × 1.2°	Giorgi et al. (2012)
		MPI-ESM-MR	1.9° × 1.9°	
		NorESM1-M	2.5° × 1.9°	
REMO2015	REMO	HadGEM2-ES	1.9° × 1.2°	Teichmann et al. (2020)
		MPI-ESM-LR	1.9° × 1.9°	
		NorESM1-M	2.5° × 1.9°	

Medium-Range Weather Forecasts. The analysis is produced with a 1 hr time-step, using a 4D-Var assimilation scheme. Data are provided on 137 vertical levels up to 0.01 hPa (Hersbach et al., 2020). Although ERA5 has evidenced some differences in the representation of surface variables compared to observational records from meteorological stations, it was found to adequately represent the spatial patterns and long-term variability of climate extremes in large portions of SA (Balmaceda-Huarte et al., 2021). This data set is one of the few gridded products available for both variables of interest at a daily scale and for the climatological reference period over SA, while its relatively high spatial resolution makes it suitable to compare with the RCM outputs. As an additional sensibility analysis, the representation of climate extremes by ERA5 was compared to another observational product to consider observational uncertainty, which is a known issue over SA (Condom et al., 2020; Sun et al., 2018). The CPC Global Unified daily gridded data set (CPC, Xie et al., 2007), which is constructed using in-situ information and corrections through satellite data and is available at 0.5° of spatial resolution.

In terms of numerical models' simulations, two CORDEX-CORE RCMs are available for both variables of interest: REMO2015 (Remedio et al., 2019) and RegCM4v7 (Giorgi et al., 2012) at a spatial resolution of 0.22°. Three earth system model-regional climate model combinations comprise the CORDEX-CORE model ensemble (Table 1). Besides considering the historical model outputs (1981–2010) and given that reliable knowledge on the future climate change signal (CCS) of compound extremes is necessary for adaptation and mitigation strategies, the future projections of the Representative Concentration Pathways (RCPs) 2.6 and 8.5 low and high-emission scenarios (Moss et al., 2010) were considered to analyze the expected changes in a context of global warming. Specifically, the 30-year period 2070–2099 (late 21st century) was selected to assess the CCS. To perform a spatially consistent analysis, these data were regridded to the same 0.25° resolution of the ERA5 data. The ESMs from the *Coupled Model Intercomparison Projects Phase 5* (CMIP5) (Taylor et al., 2012) used to drive the higher-resolution models—outlined in Table 1—were also employed and compared in this work, all of them regridded into a common grid of 2°.

2.2. Methods

2.2.1. Definition of Hazards

Following the methodology employed in the assessment of CE over Africa by Weber et al. (2020), the time-series of these events were estimated in ERA5 and the different model outputs for their historical and future scenarios. The individual events used to study the compound extremes were:

1. *HWs*: when Tx was above its 95th percentile (estimated during the reference period) for at least three consecutive days.
2. *Extreme Rainfall (ER)*: when Pr was above its 95th percentile, estimated during the rainy days (greater or equal to 1 mm/day) of the reference period.
3. *Dry-Spells (DSs)*: when Pr was less than 1 mm/day for at least five consecutive days.

Different studies have addressed the evaluation of dry conditions over SA and have considered different methodologies for this purpose, usually working at a monthly or seasonal time-scale, and including some commonly used indices such as the *Standard Precipitation Index* and the *Standard Precipitation-Evaporation Index* (de Madeiros et al., 2022; Iacovone et al., 2020; Libonati et al., 2022; Penalba & Rivera, 2016) and also some

Table 2
Compound Events Definitions, Following the Work by Weber et al. (2020)

Type of occurrence	Definition	Combination	Acronym
Coincident	Simultaneous occurrence of the individual events for at least 1 day (same day or days)	Heatwaves and extreme rainfall	HW + ER.c
		Heatwaves and dry-spells	HW + DS.c
Sequential	One individual event occurs after the other (considering a time period from 1 day and up to 7 days).	Heatwaves and extreme rainfall	HW + ER.s
		Heatwaves and dry-spells	HW + DS.s
		Dry-spells and extreme rainfall	DS + ER.s

simplified estimations such as dry-day frequencies (Espinoza et al., 2019). In the present study, we account for dry sequences with a minimum required length to guarantee meteorological dry conditions, such as in Weber et al. (2020) working with CEs over Africa. It is important to mention that, to evaluate the incidence of the minimum number of dry days used to define a dry-spell in the CE results, a sensibility analysis was performed, varying this threshold from 5 to 10 days. Even though the quantity of CE was clearly reduced when lengthening the DSs, the general spatial pattern of CE and their future projections did not change, with the same areas being affected by these climate hazards (not shown). Hence, any policy making informed by these results would still focus on the same areas independently of this methodological choice.

The occurrence of CE as defined in this study comprises the combination of two different individual events as described above, that can occur coincidentally (simultaneously, in at least 1 day) or sequentially within a certain time-period (up to 7 days). These definitions represent multivariate and temporally compounding climate events, respectively, which can contribute to socio-economic and environmental risk and population exposure (Hao et al., 2018; Zscheischler et al., 2018). In this way, the different CE evaluated here (Table 2) were estimated from the ERA5 reference data set, the CPC data set and for each climate model (RCM and ESM) and scenario.

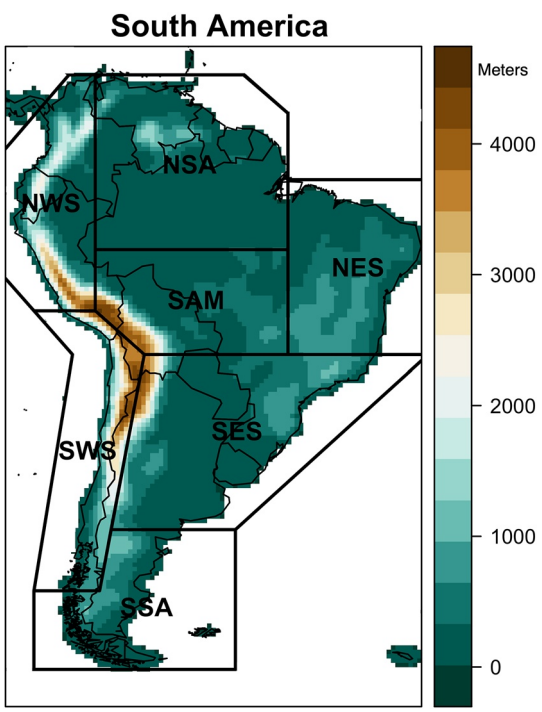

Figure 1. South American continent. Shaded contours indicate the topography as depicted by ERA5 (in meters). The seven sub-regions over South America according to the Intergovernmental Panel on Climate Change sixth report (adapted from Iturbide et al., 2020) are also plotted: NWS, Northwestern South America; NSA, Northern South America; SAM, South American Monsoon; NES, Northeastern South America; SWS, Southwestern South America; SES, Southeastern South America; SSA, Southern South America.

2.2.2. Evaluation Framework

In a first step, the representation of the individual events considered to detect the occurrence of CE was evaluated in ERA5 and in each model simulation for the current climate conditions (1981–2010 reference period). RCM and ESM ensembles of biases were constructed for the sake of conciseness (the RCM and ESM ensembles have six and five members, respectively). Particularly, the extreme percentiles and climatological patterns of the individual events were studied. Note that for the ESMs biases, the ERA5 reference was used in the same grid resolution as the ESMs, that is, 2°.

In the following step, the CE assessment was performed based on their mean annual frequency (number of CE) and duration (in the case of coincident events, the persistence of CE as depicted by the number of consecutive days identified with a CE). The CCS under the RCP 2.6 and 8.5 scenarios was analyzed in terms of the difference in the frequency and duration of CE during the late 21st century (2070–2099), compared to the reference period. Additionally, model uncertainty in the future projections was addressed through a signal-to-noise analysis. To test the robustness of the results, the average change of the RCM ensemble was compared to the standard deviation computed within each ensemble member. Therefore, if the absolute value of the ratio between the average change and the standard deviation was greater than one, then these *robust* changes as depicted by the RCM ensemble can be considered different from the noise associated with the inter-model variability (Coppola et al., 2021).

To obtain regional summarized results, the seven sub-regions selected over SA for the latest IPCC report were used (Iturbide et al., 2020). This enables

us to provide specific regional climatic information useful for decision makers and stakeholders. Furthermore, to ease the interpretation of the results, a topographical map of SA with the different IPCC climatic regions is provided in Figure 1.

3. Results and Discussions

3.1. Individual Events

Initially, the main features of the individual events considered to define the CE occurrence were explored over SA. Figure 2 (top panels) presents the 95th percentile of Tx—during the 1981–2010 reference period—used as threshold to define a HW (when Tx is above this value for, at least, three consecutive days). For brevity, results are plotted for the REMO and RegCM RCM ensembles, separately. Results for the ESMs ensemble are also presented for comparative purposes, whereas the performance of the individual ESMs is available in Figure S1 in Supporting Information S1 (see Supporting Information S1). East of the Andes, the maximum temperatures were found according to the observations over South American Mooson (SAM), decreasing to the Atlantic coast and presenting the minimum values in Southern South America (SSA) (Figure 2, top row, left panels). The presence of the Andes orographic barrier was evident mainly in the RCM ensembles, which presented an intense zonal gradient in the proximity of the Andes, indicating the minimum values of this percentile over the highest areas of Perú, Bolivia, and Argentina. The ESMs ensemble exhibited a more homogeneous spatial pattern due to their

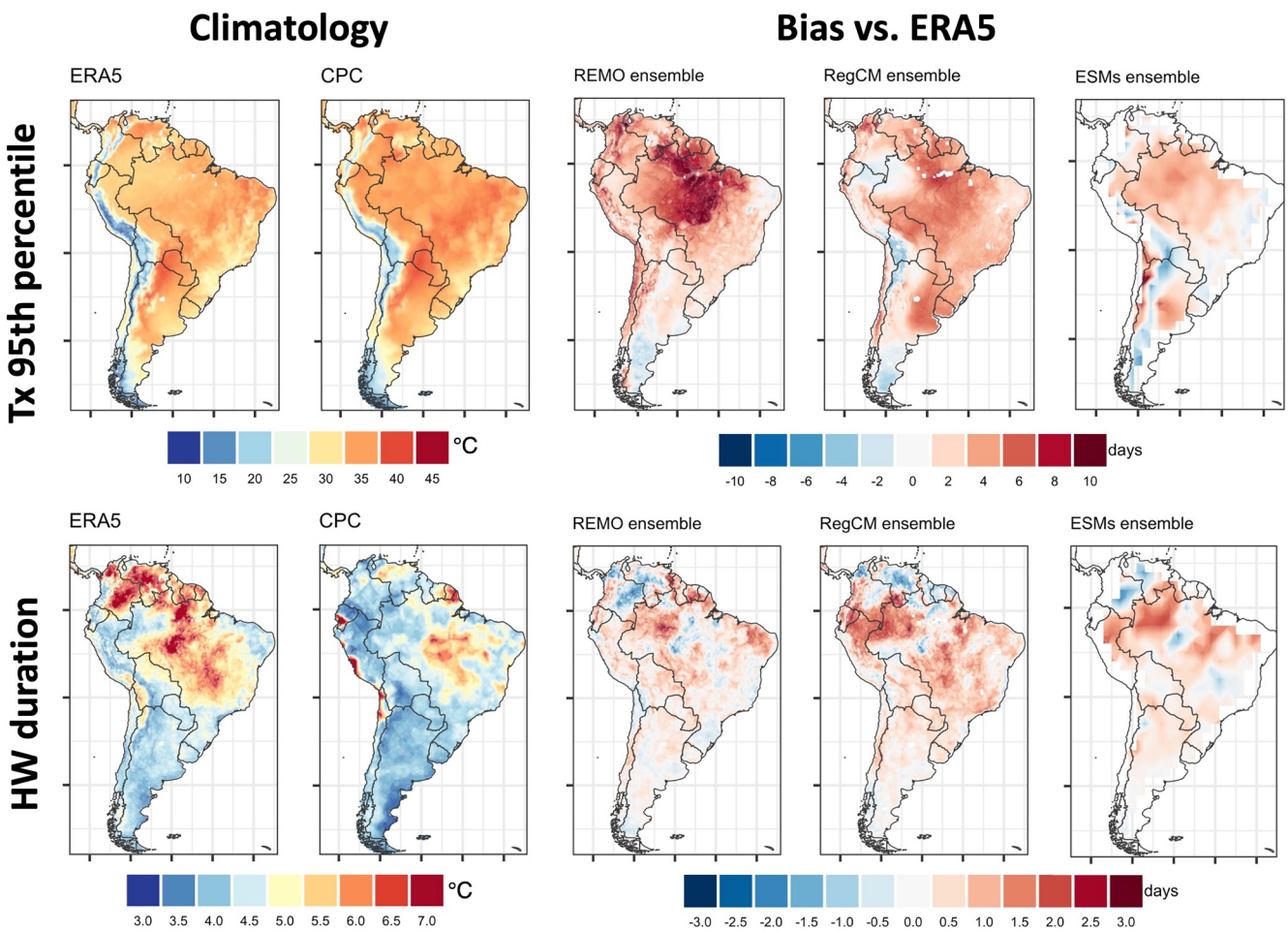

Figure 2. Main features of temperature-related events during the reference period 1981–2010: 95th percentile of daily maximum temperature (Tx, top row); heatwave duration (bottom row). The maps in the left panels show the mean climatological fields for the ERA5 and CPC Global Unified daily gridded data sets, while the right panels display the model biases with respect to the ERA5 reference. Results are plotted for the REMO and RegCM regional climate models and for the driving earth system models ensembles, separately.

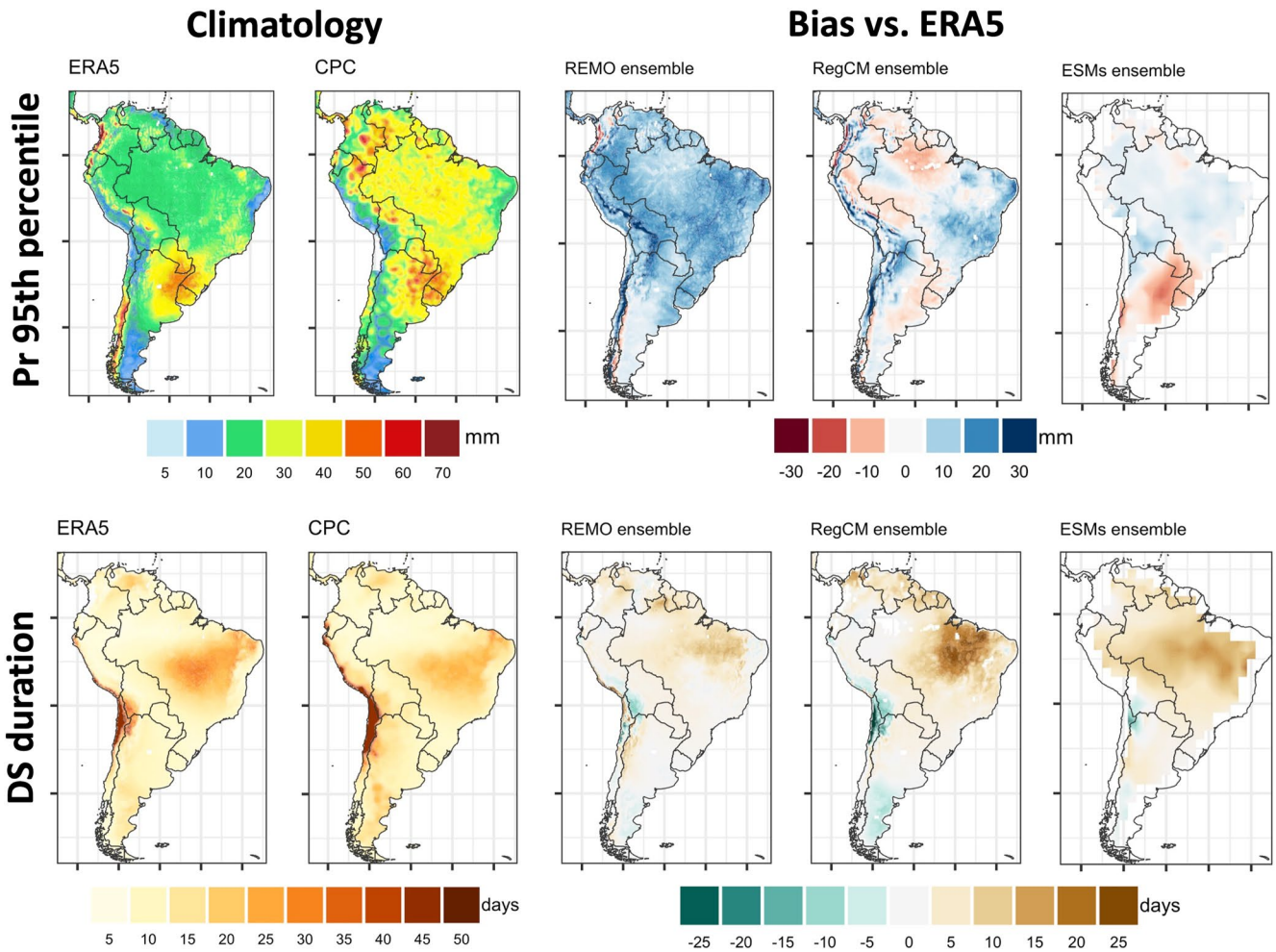

Figure 3. Main features of precipitation-related events during the reference period 1981–2010: 95th percentile of daily precipitation (Pr, top row); dry-spells duration (bottom row). The maps in the left panels show the mean climatological fields for the ERA5 and CPC Global Unified daily gridded data sets, while the right panels display the biases with respect to the ERA5 reference. Results are plotted for the REMO and RegCM regional climate models and for the driving earth system models ensembles, separately.

lower resolution, not being able to capture the Tx spatial variability related to the Andes and over the rest of SA and highlighting the added value of RCM simulations in depicting these features.

In terms of model biases (Figure 2, top row, right panels), both RCMs tended to overestimate the 95th percentile of Tx, particularly REMO over Amazonia Northern South America (NSA) and RegCM also over southeastern South America (SESA, part of SES), in agreement with results by Coppola et al. (2021) for warm extreme indices. This last RCM ensemble showed an underestimation of extreme temperatures over the Andes and in some areas of the Amazonia (parts of Northwestern South America [NWS] and Northern South America [NSA]). The ESMs also depicted intense and spatially varied biases in SSA, probably related to a misrepresentation of the Andes topography.

The persistence of these extreme temperature conditions is reflected in the maps of HW duration of Figure 2 (bottom row, left panels), where the maximum durations were found over central Brazil and northern SA (SAM and Northeastern South America [NES]), larger in ERA5 than in CPC, and were of about 6–7 days in the RCM ensembles. Both RCM ensembles similarly reproduced this feature, slightly overestimating the HW duration over SA and presenting more discrepancies with the ERA5 reference in NSA and SAM, which were congruent with the bias patterns of the driving ESMs. Note that the overestimation of HW duration in the ESM ensemble over

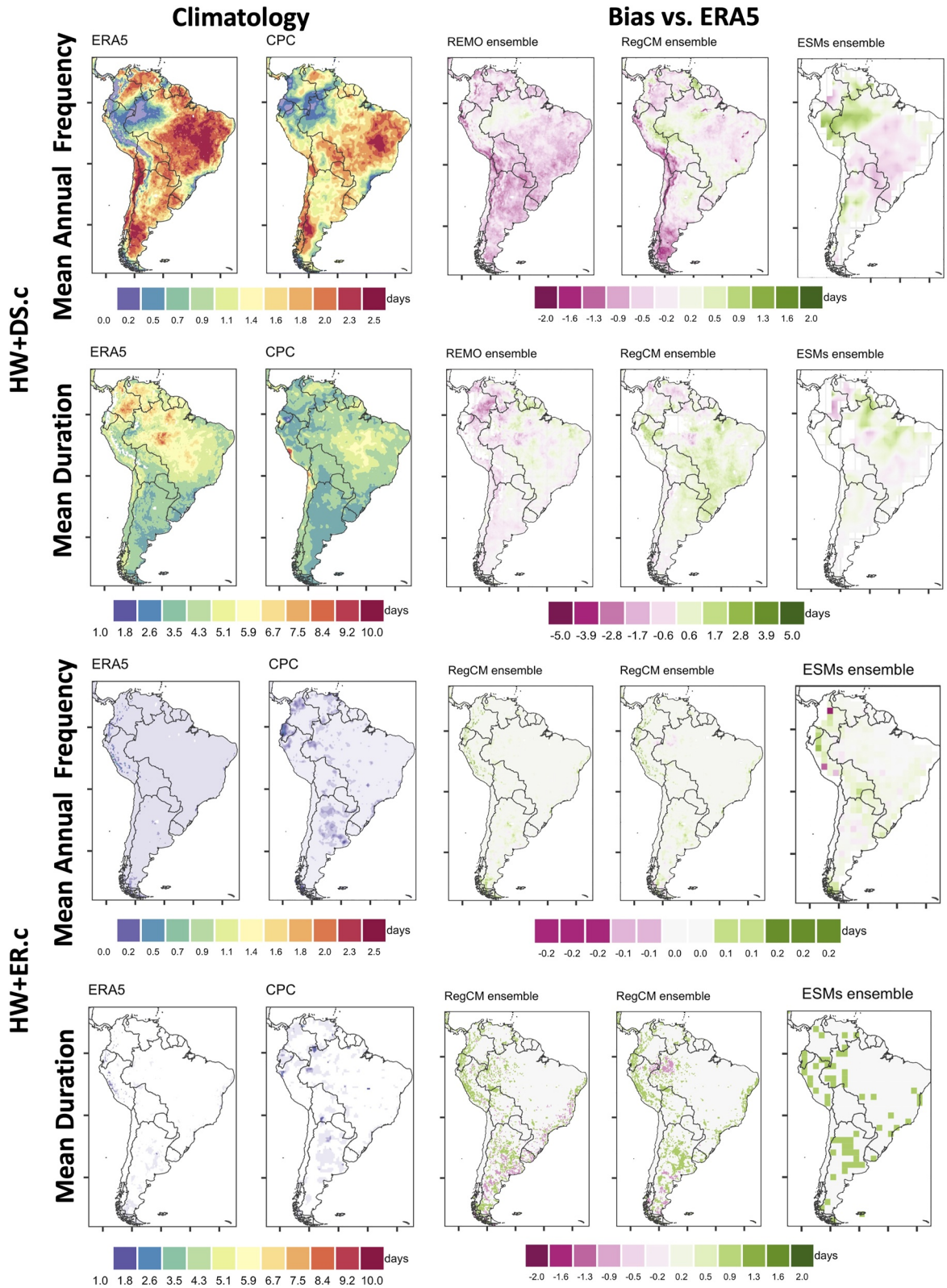

Figure 4. Mean annual frequency and mean duration of coincident heatwaves (HWs) and dry-spells and coincident HWs and extreme rainfall (HW + DS.c and HW + ER.c, respectively) during the reference period 1981–2010. The maps in the first and third row show the mean climatological fields and the second and fourth rows display the biases with respect to the ERA5 reference. Results are plotted for the REMO and RegCM regional climate models and for the driving earth system models ensembles, separately.

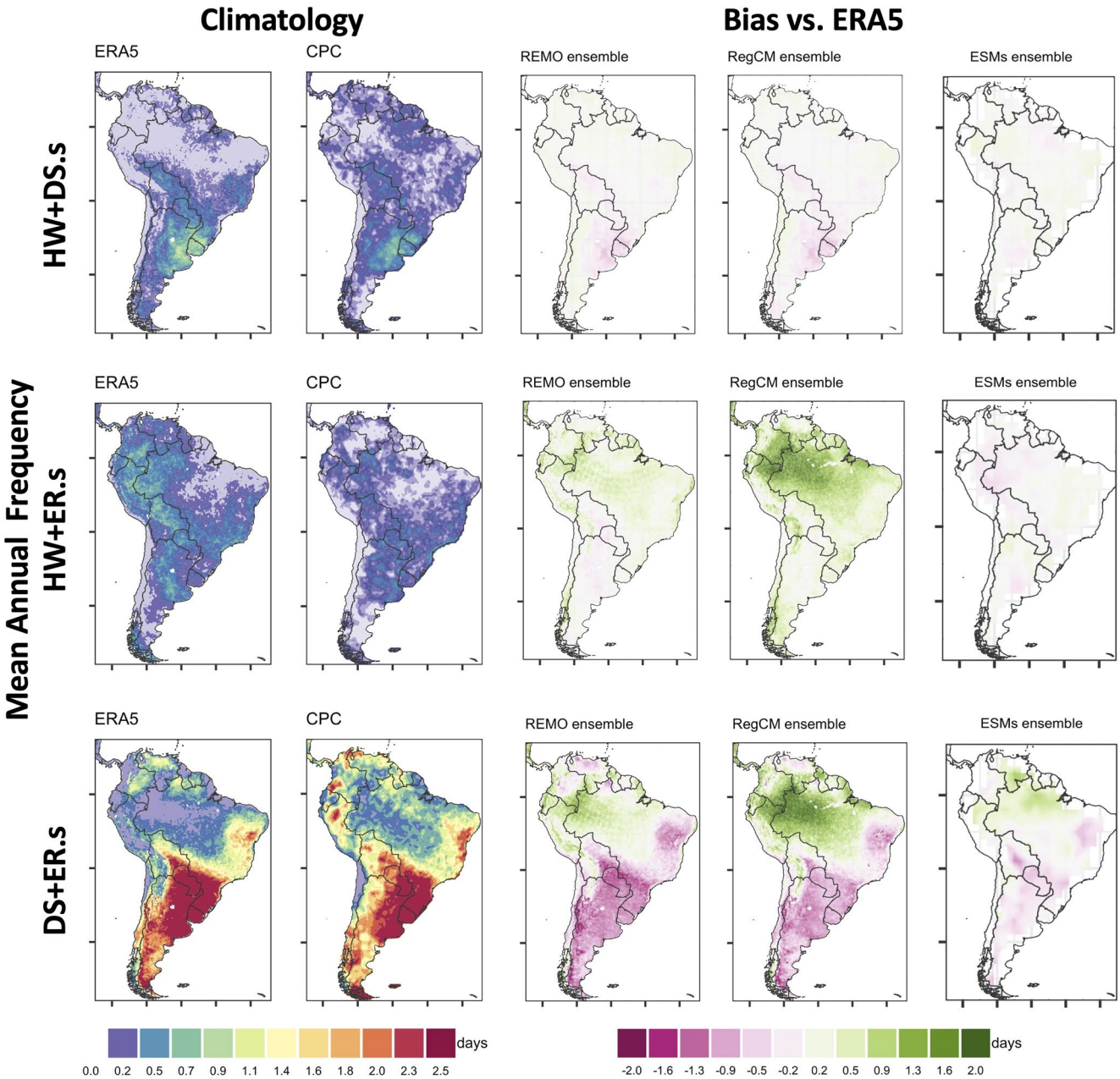

Figure 5. Mean annual frequency of sequential compound events (heatwaves [HWs] and dry-spells (DSs), HWs and extreme rainfall (ER), DSs and ER) during the reference period 1981–2010. The maps in the top row show the mean climatological fields and the bottom row displays the biases with respect to the ERA5 reference. Results are plotted for the REMO and RegCM regional climate models and for the driving earth system models ensembles, separately.

these areas was present in all the individual ESMs but in HadGEM2-ES, which showed an opposite bias over these regions (see Figure S1 in Supporting Information S1).

Similarly, some features of precipitation-related events are displayed for extremely wet and dry conditions (Figure 3, top and bottom rows, respectively). Results of the individual ESMs are presented in Figure S2 in Supporting Information S1. The spatial distribution of ER as depicted by the 95th percentile of Pr (estimated for the period 1981–2010, considering rainy days only) is presented in Figure 3 (top row). Maxima was found over SESA and the Amazon basin, although ERA5 presented lower values over this last region than CPC. REMO overestimated the extreme intensities over all SA—and especially in the proximity of the Andes—whereas RegCM showed a more heterogeneous pattern of biases, underestimating this Pr feature over SESA and parts of the

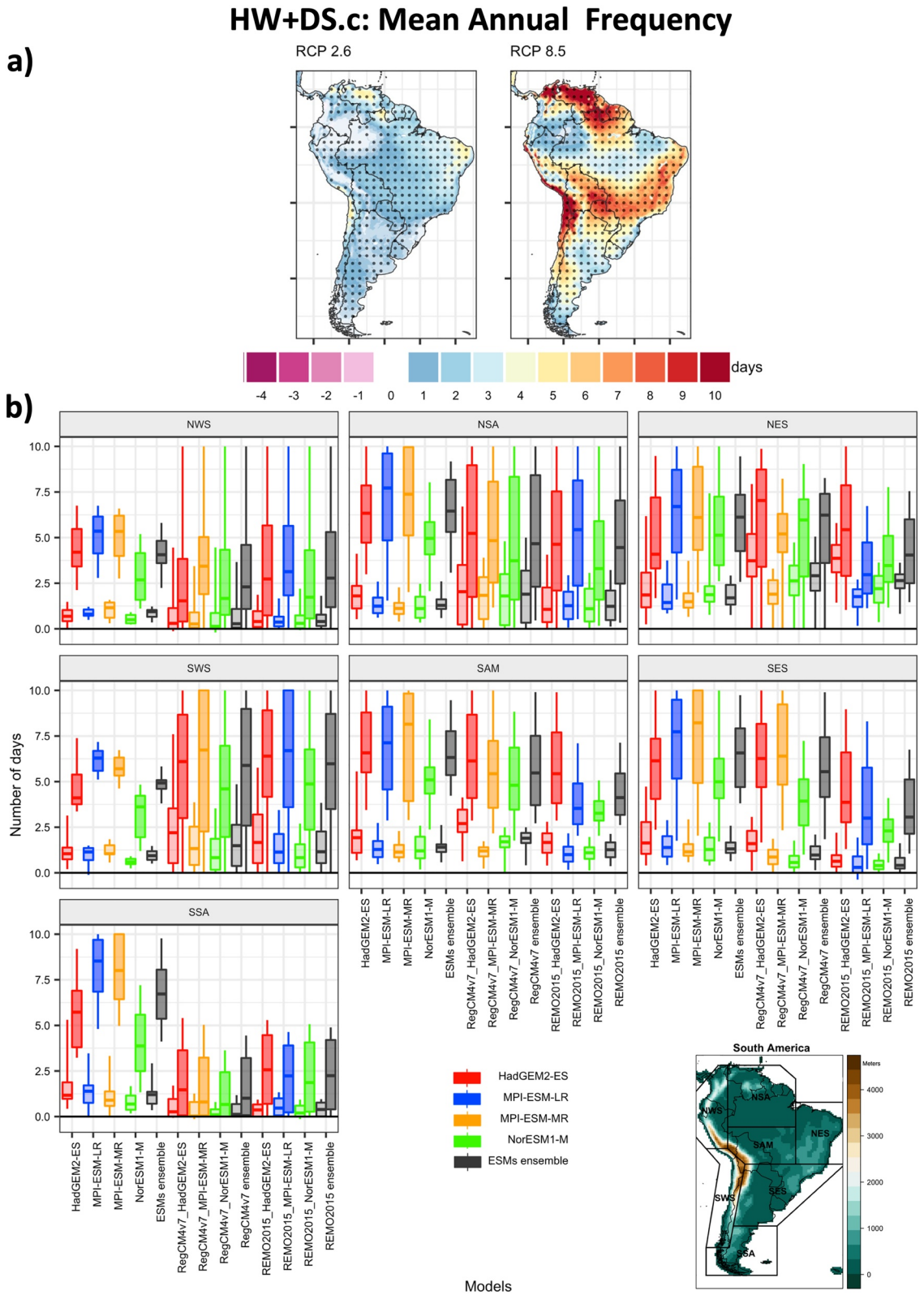
HW+DS.c: Mean Annual Frequency
a)
RCP 2.6
RCP 8.5
days
-4 -3 -2 -1 0 1 2 3 4 5 6 7 8 9 10
b)
NWS
NSA
NES
SWS
SAM
SES
SSA
Number of days
HadGEM2-ES
MPI-ESM-LR
MPI-ESM-MR
NorESM1-M
ESMs ensemble
RegCM4v7_HadGEM2-ES
RegCM4v7_MPI-ESM-MR
RegCM4v7_NorESM1-M
RegCM4v7 ensemble
REMO2015_HadGEM2-ES
REMO2015_MPI-ESM-LR
REMO2015_NorESM1-M
REMO2015 ensemble
Models
South America
Meters

Figure 6.

Amazonia (NSA and SAM) compared to the ERA5 reference. RCMs depicted remarkably larger values of this percentile than the driving ESMs, mostly due to a differentiated representation of convective activity that plays a major role enhancing ER events (Rasmussen & Houze, 2016; Salio et al., 2007). This wet bias identified in the ESM-driven RCM simulations is consistent with results from Olmo and Bettolli (2021) who pointed out the overestimation of Pr—particularly in extremes—in the CORDEX-CORE RCM evaluation runs, that is, driven by reanalysis data. Furthermore, the overestimation of orographic precipitation is a well-known feature of the RCMs over the Andes (Bettolli et al., 2021; Remedio et al., 2019; Teichmann et al., 2020). The ESMs showed their largest underestimation over SES (the greatest by NorESM1-M as illustrated in Figure S2 in Supporting Information S1), which has been highlighted in the literature as one of the hotspots for heavy rainfall events in terms of their frequency and intensity and their related impacts (Bettolli et al., 2021; Cavalcanti et al., 2015).

Moving to the DSs evaluation (Figure 3, bottom row), the persistence of these events in the reference data set was found to be larger over central and northeastern Brazil (SAM and NES) than in the rest of SA, excluding northern Chile (north of Southwestern South America [SWS]) where the Atacama Desert is located, and rain occurrence is rare. NES is characterized by rainfall scarcity and has been the scene of multiple major droughts, typically associated with large-scale phenomena such as El Niño, a northward displacement of the Intertropical Convergence Zone and wind motion anomalies affecting the descending branch of the Walker circulation (de Medeiros et al., 2020). In this regard, the DS duration maxima over Brazil (portions of SAM and NES) was overestimated in all model ensembles but more pronounced in RegCM which, in addition, presented greater biases compared to ERA5 over the Andes and in Argentinian Patagonia (SSA).

This preliminary evaluation of the individual events involved in the CE occurrence results helpful to understand the spatio-temporal variability of CE and to characterize model performance in the different cases, which will be discussed in the following section.

3.2. Compound Events

The characterization of coincident CE is presented in Figure 4. Results of the individual ESMs are available in Figure S3 in Supporting Information S1. The maximum frequencies of HWs and DSs (HW + DS.c) were observed over central-eastern Brazil and SESA (portions of SAM, NES, and SES)—generally more than two events per year—which were the areas of SA that also depicted the highest extreme Tx values and the longest duration of the individual events (Figure 2). Whereas the minimum values were identified in western Amazon and NSA, with almost null frequencies. The comparison between ERA5 and CPC showed a good agreement among both data sets, although ERA5 depicted larger maximum frequencies than CPC. REMO generally underestimated the mean annual frequencies and RegCM presented a more varied pattern of biases comparable to the ESMs ensemble but exhibiting some overestimations east of the Andes of about 0.9 days. Again, HadGEM2-ES differed from the other ESMs as it tended to underestimate the HW + DS.c frequency over SAM and NSA (Figure S3 in Supporting Information S1). Moreover, the Argentinian and Chilean Patagonia—in SWS and SSA—showed a relative maximum, which was underestimated by the RCMs in about 2 days. In terms of CE duration, the center of maximum lengths—of about 6–8 consecutive days—was found over central Brazil (SAM), located a little to the east than the region with the maximum frequencies. Both RCM ensembles well-simulated the spatial distribution of this index, while RegCM tended to overestimate the durations over SES and SAM.

In the case of coincident HWs and ER (HW + ER.c in Figure 4), the frequency of these events is almost nule throughout the continent, with an average of less than 0.5 events per year as the maximum values over SSA. This was probably due to heavy precipitation occurring commonly after extreme warm conditions, that provide the instability needed for the rainfall episode and the temperature decrease afterward (Tencer et al., 2016). Given the short mean duration of HW + ER.c, model biases are sensible to small differences, showing slight overestimations by the RCMs in the areas where these models present more frequent HW + ER.c, whereas the pattern for the

Figure 6. Projected changes under the Representative Concentration Pathway (RCP) 2.6 and 8.5 scenarios during the late 21st century (2070–2099) for the mean annual frequency of coincident heatwaves and dry-spells (HW + DS.c): (a) Maps of changes, expressed as the difference in the number of days compared to the reference period (1981–2010) based on the Coordinated Regional Climate Downscaling Experiment-Coordinated Output for Regional Evaluation regional climate model (RCM) ensemble. Black dots indicate areas where the change signal is robust; (b) Boxplots of the changes for the individual RCMs and their driving earth system models (ESMs), separated according to the seven Intergovernmental Panel on Climate Change regions. Boxes indicate the 25th, 50th and 75th percentiles and their whiskers show the 5th and 95th percentiles and were created in the native model resolutions. Colors indicate the different ESMs, whereas the ensembles are presented in gray. Light and dark tones indicate the RCP 2.6 and 8.5 scenario (left and right, respectively).

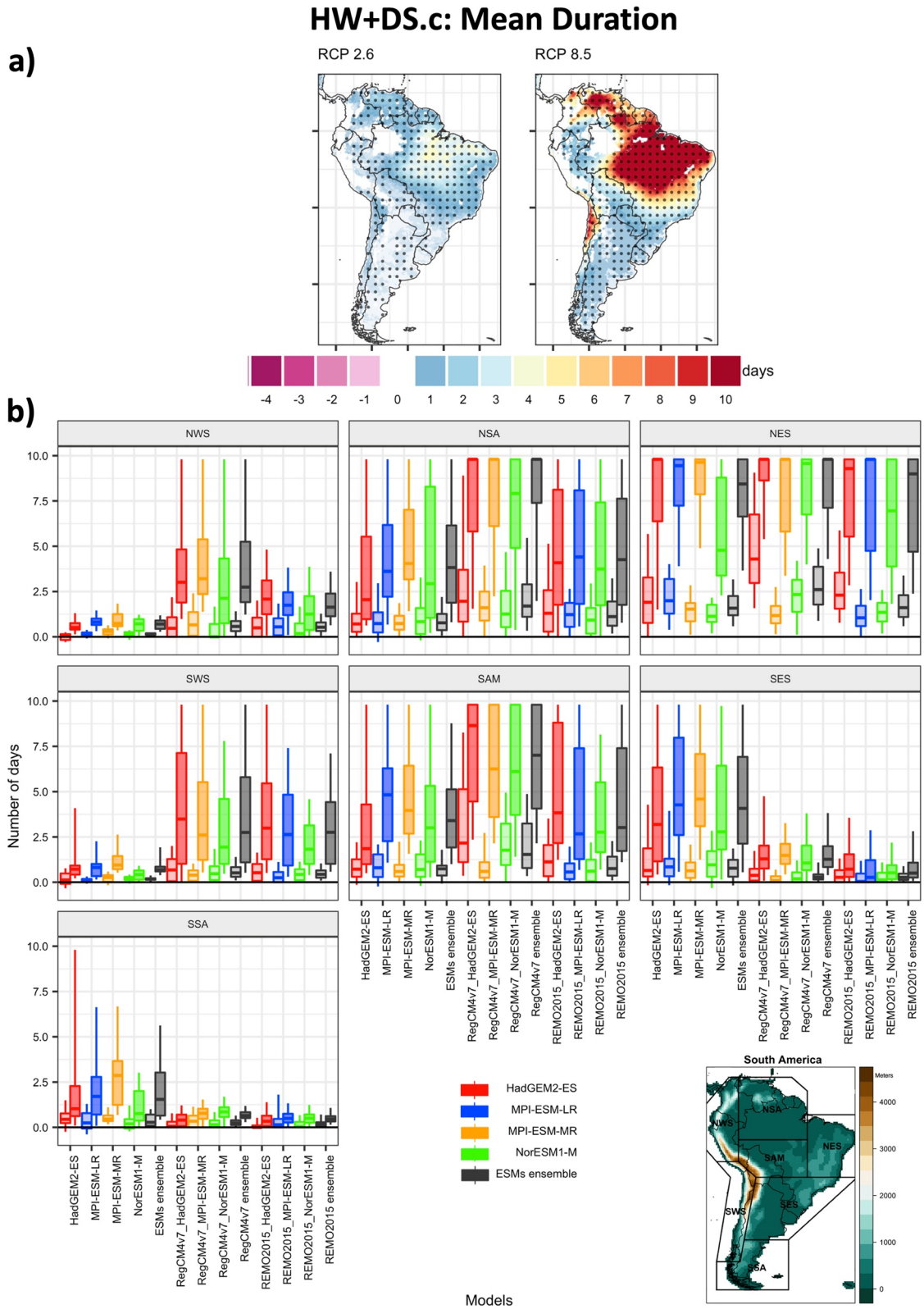
HW+DS.c: Mean Duration
a)
RCP 2.6
RCP 8.5
days
-4 -3 -2 -1 0 1 2 3 4 5 6 7 8 9 10
b)
NWS
NSA
NES
SWS
SAM
SES
SSA
Number of days
HadGEM2-ES
MPI-ESM-LR
MPI-ESM-MR
NorESM1-M
ESMs ensemble
RegCM4v7_HadGEM2-ES
RegCM4v7_MPI-ESM-MR
RegCM4v7_NorESM1-M
RegCM4v7 ensemble
REMO2015_HadGEM2-ES
REMO2015_MPI-ESM-LR
REMO2015_NorESM1-M
REMO2015 ensemble
Models
South America
Meters

Figure 7.

ESMs ensemble was similar to the RCM results, although the pattern of slight overestimations was mainly due to the MPI-EM-LR and MPI-ESM-MR simulations (see Figure S3 in Supporting Information S1).

Results of the sequential CE assessment are presented in Figure 5, whereas the individual performances of the driving ESMs are illustrated in Figure S4 in Supporting Information S1. The joint occurrence of HWs and DSs but, in this case, sequentially (HW + DS.s), exhibited a much-reduced number of events over all SA (Figure 5, first row) when compared with the coincident CE of Figure 4. The maximum average annual frequencies were of about 1 in ERA5 over SES and near 0.5 in the rest of SA, like CPC. These smaller frequencies in the sequential CE may be due to the temperature-precipitation interaction, as the atmospheric feedback between dry conditions and warm temperatures occurring together—that is, simultaneously—mainly promotes the simultaneous occurrence of this CE. Both RCM ensembles depicted similar performances, slightly underestimating the frequencies over SES, like the ESMs.

The HWs and ER sequential CE (HW + ER.s) showed larger frequencies in most of the continent than the coincident event, with maximum values over NWS as depicted by ERA5 (see Figure 5, second row), which is related to the warm and humid conditions and the intense rainy season there (Espinoza et al., 2021). CPC reproduced this spatial pattern similarly, but with smaller frequencies over northwestern SA. Despite showing larger biases than the driving ESM ensemble, the RCMs evaluation was more satisfactory in terms of CE frequencies for the REMO ensemble, since RegCM presented higher and extended overestimations over this area.

The last sequential CE assessed here was the occurrence of DSs followed by an ER event (DS + ER.s in Figure 5, third row), being SES the main hotspot for this CE. ERA5 and CPC agreed in their representation of this CE, although ERA5 did not detect the maximum frequencies in some areas of NWS shown in the CPC data set. RegCM identified a clearly overestimated maximum center over NWS, which was not observed in the REMO ensemble. Particularly over SES and SSA, the RCMs notably underestimated these values, with a bias of more than 1 day per year. In this case, although the differences with respect to ERA5 seemed more intense in the RCM ensembles than in the ESMs for specific regions of SA, both ensembles identified the same areas as hotspots for CE occurrence. As presented in Figure S4 in Supporting Information S1, NorESM1-M strongly overestimated DS + ER.s frequency over SES—in accordance with its underestimation of ER intensities discussed in Section 3.1—whereas the MPI models showed large overestimations through NSA. Note, however, that the ESMs provide much less spatial detail—which is one clear benefit of the higher-resolution RCMs—and the differences in grid resolution may interfere in the biases values.

3.3. Climate Change Signal

For the assessment of the expected changes on CE during the late 21st century (2070–2099), the CCS was estimated as the difference between the mean annual frequency (or duration) in this future period and in the 1981–2010 reference. Focus was put on the CE that were the most remarkable in the historical evaluation, presenting the largest frequencies in different areas of SA.

Figures 6a and 7a show the results for the projected frequency and duration, respectively, of coincident HWs and DSs CE (HW + DS.c) in the ensemble of all CORDEX-CORE RCMs over SA. The areas where the signal was higher than the noise within the model ensemble are dotted, and those changes are hereinafter mentioned as robust (see Section 2.2 for more details). For more insight, Figures 6b and 7b synthesize in boxplots the CCS in each individual RCM and in their driving ESMs, which was replicated for the RCP 2.6 and 8.5 scenarios and for each of the seven IPCC sub-regions over SA.

HW + DS.c are projected to be more frequent in the late 21st century, especially in NSA, northern Chile (north of SWS) and large areas of SES. These changes are notably larger when considering the worst-case scenario (RCP 8.5), with expected increases close to 10 days per year. The duration of this CE showed future increments

Figure 7. Projected changes under the Representative Concentration Pathway (RCP) 2.6 and 8.5 scenarios during the late 21st century (2070–2099) for the mean duration of coincident heatwaves and dry-spells (HW + DS.c): (a) Maps of changes, expressed as the difference in the number of days compared to the reference period (1981–2010) based on the Coordinated Regional Climate Downscaling Experiment-Coordinated Output for Regional Evaluation regional climate models (RCM) ensemble. Black dots indicate areas where the change signal is robust; (b) Boxplots of the changes for the individual RCMs and their driving earth system models (ESMs), separated according to the seven Intergovernmental Panel on Climate Change regions. Boxes indicate the 25th, 50th, and 75th percentiles and their whiskers show the 5th and 95th percentiles and were created in the native model resolutions. Colors indicate the different ESMs, whereas the ensembles are presented in gray. Light and dark tones indicate the RCP 2.6 and 8.5 scenario (left and right, respectively).

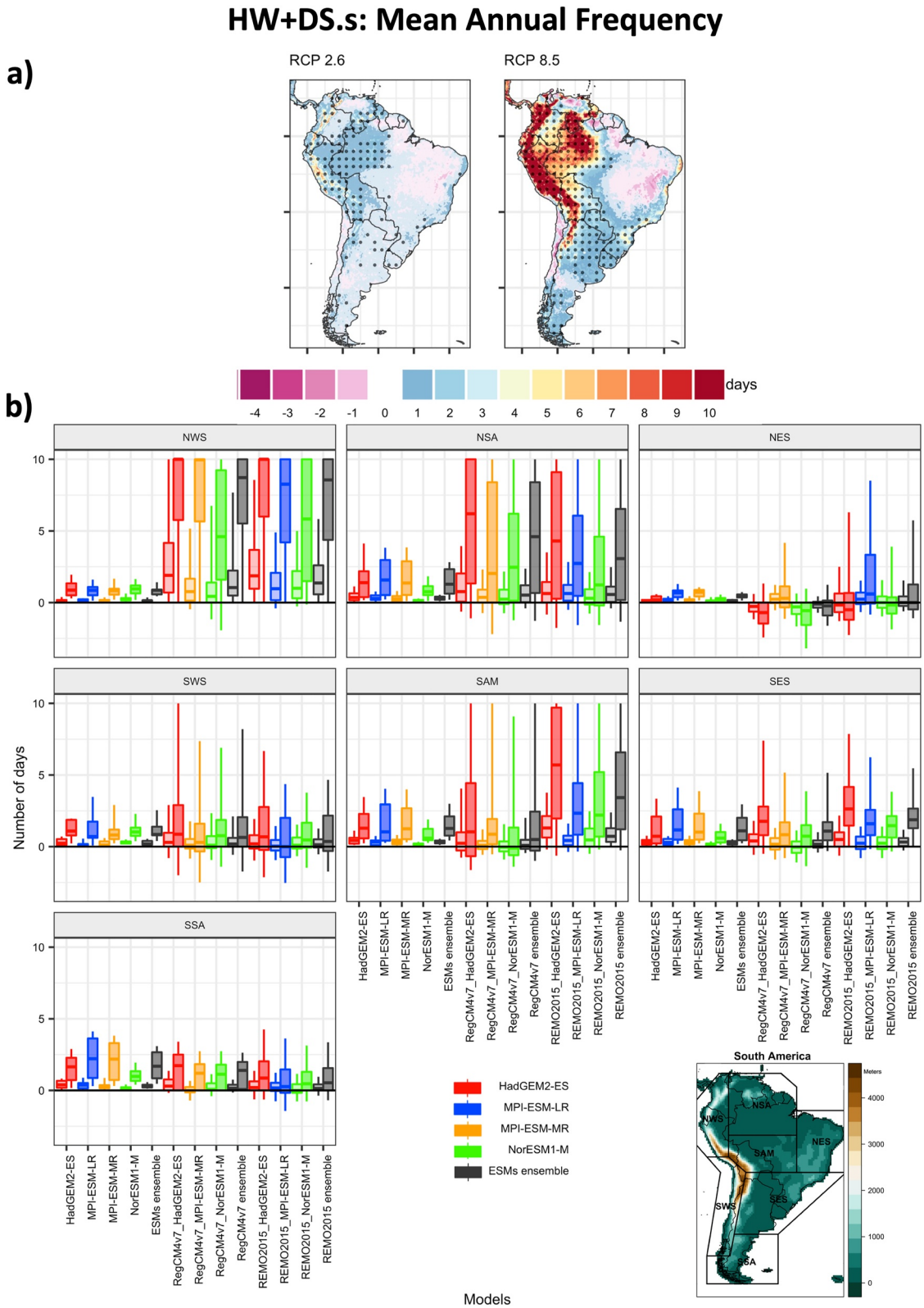
HW+DS.s: Mean Annual Frequency
a)
RCP 2.6
RCP 8.5
-4 -3 -2 -1 0 1 2 3 4 5 6 7 8 9 10
days
b)
NWS
NSA
NES
SWS
SAM
SES
SSA
Number of days
HadGEM2-ES
MPI-ESM-LR
MPI-ESM-MR
NorESM1-M
ESMs ensemble
RegCM4v7_HadGEM2-ES
RegCM4v7_MPI-ESM-MR
RegCM4v7_NorESM1-M
RegCM4v7 ensemble
REMO2015_HadGEM2-ES
REMO2015_MPI-ESM-LR
REMO2015_NorESM1-M
REMO2015 ensemble
Models
South America
Meters

Figure 8.

particularly over NES and extended to NSA—clearly intensified in RCP 8.5—whereas only slight differences between both emission scenarios were found in the rest of the continent. The RCM ensemble results for both the frequency and duration of HW + DS.c were robust over most of SA, evidencing a good agreement among RCM simulations. It is worth mentioning that the projected increases in HW + DS.c over NSA and NES agree with the observed changes of individual events documented in the literature, indicating an intensification of the extreme warm conditions and a decline in precipitation amounts (Dereczynski et al., 2020; Regoto et al., 2020). Moreover, even though the changes are smaller over SES, the robust increases in this CE follow the detected upward trends in warm extremes in the historical period. Whereas the precipitation changes are more variable and season-dependent over the region, with more heterogeneous changes in dry conditions and increases in ER events that are projected to intensify in the future (Ceron et al., 2020; Dereczynski et al., 2020; Olmo et al., 2020; Regoto et al., 2020).

When analyzing each individual model simulation (Figures 6b and 7b), both the frequency and duration of HW + DS.c tended to present more spatial variability in RCP 8.5 than in RCP 2.6, as depicted by the larger boxes. In the case of the frequency (Figure 6b), the main CCS of the driving ESMs was generally conserved in the RCM simulations—as can be observed, for instance, in the median of the changes of NSA, SWS and SES, the highlighted areas in Figure 6a—although the higher-resolution models added spatial detail in the results and therefore they depicted larger variability in the boxplots. Although the signal-to-noise analysis discussed in Figure 6a showed a general good agreement among the different simulations, the change rate presented some differences among models in specific regions: the REMO ensemble exhibited less changes than RegCM such as in SAM and SES, whereas the NorESM1-M ESM and its corresponding RCMs tended to show more reduced changes than the rest of the simulations. Furthermore, the CCS in the southern tip of the continent (SSA) depicted larger positive changes in the ESMs than in the RCMs, particularly for the high-emission scenario. Hence, there is some level of model uncertainty in the projections of HW + DS frequency, especially at the regional scale, which motivates the use of high-resolution data to assess these local changes but keeping in mind the possible deviations from the coarse-resolution models. In the case of HW + DS.c duration changes (Figure 7b), the RCM ensembles presented greater (lower) changes and more spatial variability than the ESMs over NWS and SWS (SWS and SES), evidencing some discrepancies between the higher-resolution models and their driving ESMs.

Similarly to the previous analysis, Figures 8a and 9a show the CCS maps for the mean annual frequency of two sequential CE: HWs and DSs (HW + DS.s) and DSs and ER (DS + ER.s). For HW + DS.s (Figure 8a), the largest and most robust increases were found over NWS, whereas slight positive and negative changes could be detected in the rest of the continent, but generally not robust enough. An intensification of the changes was evident when analyzing the worst-case scenario (RCP 8.5), especially over NWS but also in the positive (negative) changes over SSA (NES), showing more agreement among the RCM ensemble over SSA. In the case of DS + ER.s (Figure 9a), this region standed out as the main area with a robust increasing number of this CE, even in the RCP 2.6 scenario. The intensity of these changes over SES was similar in RCP 8.5 but extended over large portions of the continent. Contrarily, a reduction (though not robust) in DS + ER.s was projected over NSA—exhibiting a dipole structure in the CCS pattern over the Amazon basin—and the southern surroundings of the Andes Mountain range, particularly over southern Chile (SWS).

In addition, a more comprehensive analysis of the CCS for the frequency of HW + DS.s is provided in Figure 8b, in the same way as it was done for HW + DS.c. The RCMs depicted larger changes (and more spatial variability given the bigger boxes) than their driving ESMs in regions like NWS, NSA, SWS, and SAM, where the projected changes typically showed increases in the frequency of this CE. On the other hand, the negative changes over NES shown in the RCM ensemble (Figure 8a) was generally consistent among the individual RCM simulations, whereas their driving ESMs showed changes near zero (but with slightly positive values) and no spatial variability over the region. In this regard, the information provided by the RCMs over NES added more spatial detail and even turned the projections into negative changes in their ensemble (although not robust, according

Figure 8. Projected changes under the Representative Concentration Pathway (RCP) 2.6 and 8.5 scenarios during the late 21st century (2070–2099) for the mean annual frequency of sequential heatwaves and dry-spells (HW + DS.s): (a) Maps of changes, expressed as the difference in the number of days compared to the reference period (1981–2010) based on the Coordinated Regional Climate Downscaling Experiment-Coordinated Output for Regional Evaluation regional climate models (RCM) ensemble. Black dots indicate areas where the change signal is robust; (b) Boxplots of the changes for the individual RCMs and their driving earth system models (ESMs), separated according to the seven Intergovernmental Panel on Climate Change regions. Boxes indicate the 25th, 50th, and 75th percentiles and their whiskers show the 5th and 95th percentiles and were created in the native model resolutions. Colors indicate the different ESMs, whereas the ensembles are presented in gray. Light and dark tones indicate the RCP 2.6 and 8.5 scenario (left and right, respectively).

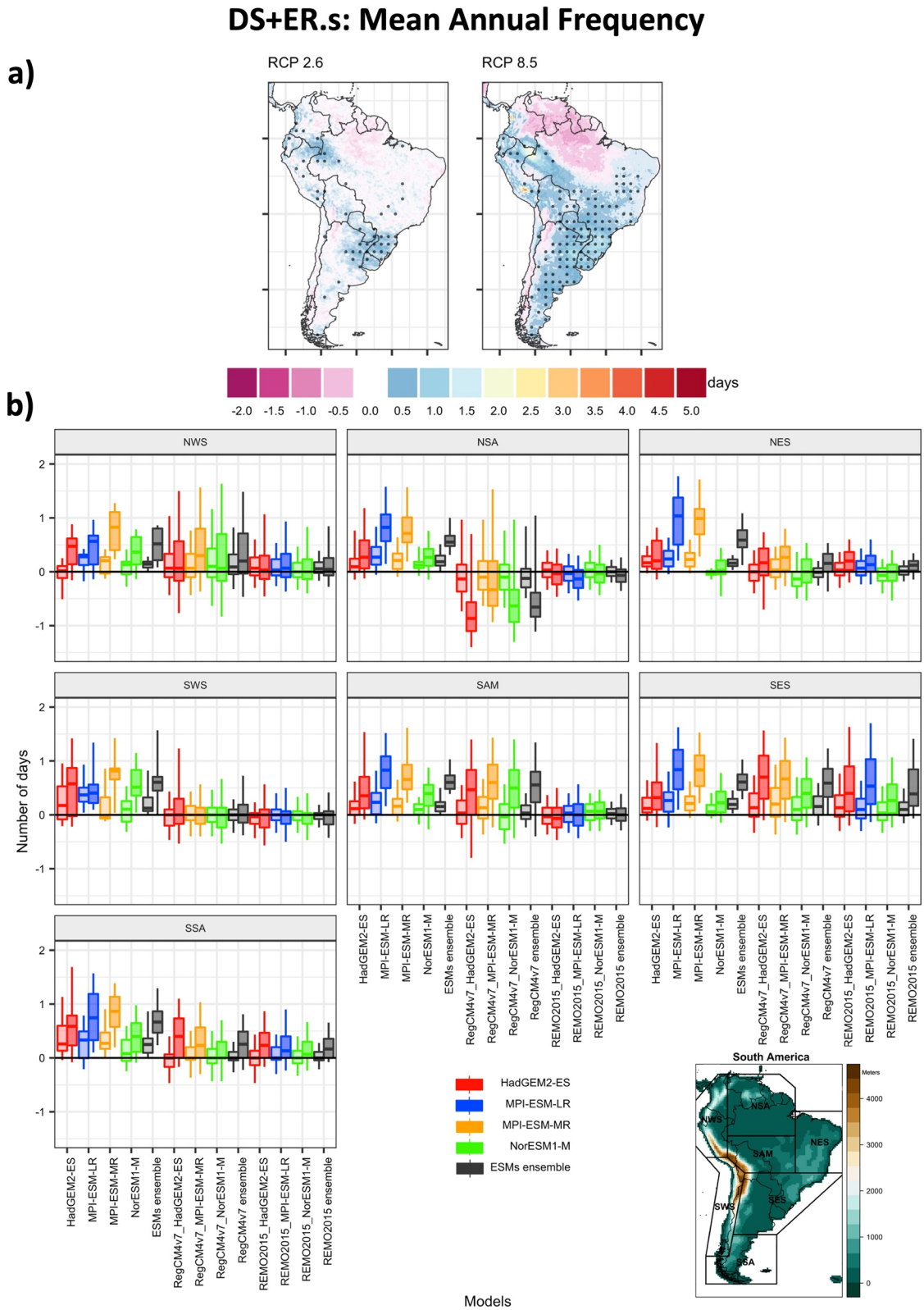
DS+ER.s: Mean Annual Frequency
a)
RCP 2.6
RCP 8.5
days
-2.0 -1.5 -1.0 -0.5 0.0 0.5 1.0 1.5 2.0 2.5 3.0 3.5 4.0 4.5 5.0
b)
NWS
NSA
NES
SWS
SAM
SES
SSA
Number of days
HadGEM2-ES
MPI-ESM-LR
MPI-ESM-MR
NorESM1-M
ESMs ensemble
RegCM4v7_HadGEM2-ES
RegCM4v7_MPI-ESM-MR
RegCM4v7_NorESM1-M
RegCM4v7 ensemble
REMO2015_HadGEM2-ES
REMO2015_MPI-ESM-LR
REMO2015_NorESM1-M
REMO2015 ensemble
Models
South America
Meters

Figure 9.

to the signal-to-noise analysis). In the case of DS + ER.s (Figure 9b), the negative changes identified in the RCM ensemble over NSA were mainly due to the RegCM simulations, which presented a general negative CCS that differed from the driving ESMs. RegCM also depicted a larger spatial spread than the REMO simulations, which did not exhibit clear changes as the median of the different simulations was around cero. This result was in line with the non-robust findings in the RCM ensemble maps illustrated in Figure 9a. In the rest of the regions, both the magnitude and the spatial spread of the CCS were in good agreement among the different ESMs and RCMs, like the increases expected over SES. Over SWS and SSA—which tended to present a reduction in the frequency of DS + ER—the comparison between ESMs and RCMs showed a lower difference in the number of days in the RCMs, with even negative values in their whiskers and boxes that were not found in their driving ESMs (compared to the reference period). This could be related to the poorer spatial resolution of the ESMs and their limitations in simulating the influence of the Andes complex topography, which can be more successfully represented by the RCM models.

4. Summary and Final Remarks

This study presents an unprecedented characterization of multiple temperature and precipitation CEs over SA, a continent with emerging economies and exposed population where extreme climate conditions are projected to intensify (IPCC, 2021). The current climate conditions (1981–2010) and future changes of CE during the late 21st century (2070–2099) were assessed using the CORDEX-CORE ensemble of RCMs over SA and their driving ESMs, considering the ERA5 reanalysis as reference. Like Weber et al. (2020), focus was put on the climatological frequency and duration of CE considering the joint occurrence of HWs, ER and DSs, which were separated in coincident (simultaneous, in at least 1 day) and sequential events (within a time-period up to 7 days). Their CCS was investigated under the RCP 2.6 and 8.5 emission scenarios.

The spatial pattern of the individual events considered to estimate the CE occurrence were adequately reproduced by the RCMs, exhibiting more discrepancies in extreme precipitation (often showing large overestimations in agreement with Olmo and Bettolli (2021)) than in the temperature-related indices, although temperature biases are also evident over SA in the different RCMs (Llopart et al., 2017; Reboita et al., 2014; Remedio et al., 2019). The influence of the Andes Mountain range in these patterns was more evident in the RCMs than in their driving ESMs, as they depicted less detail due to lower resolution, not being able to capture the spatial variability, like in the case of extreme temperatures. Although assessing the rationale behind the RCMs performance is beyond the scope of this study, it may involve some misrepresentations of convective activity and sub-grid processes, as well as regional-scale mechanisms such as the South American low-level jet (SALLJ), that is responsible for these climate extremes in regions like southeastern SA (Carril et al., 2016; Cavalcanti et al., 2015) and remote climate forcings such as El Niño-Southern Oscillation (Coelho et al., 2016) which influence is inherited from the driving ESMs.

In terms of CE, the frequency of coincident HWs and DSs—HW + DS.c—(sequential DSs and ER, DS + ER.s) was remarkable over central-eastern Brazil and southern SA (southeastern SA), whereas the other CE like coincident HWs and ER or sequential HWs and DSs depicted weak frequencies throughout the continent. Moreover, the RCMs were able to adequately reproduce the main features of CE, although with some regional differences such as a general underestimation of the maximum frequencies of these CE in northeastern Brazil and southeastern SA, respectively. These detected hotspots were in line with previous climatic observational characterizations over the continent, demonstrating the RCMs ability to capture the spatial variability of these climate extremes (Bettolli et al., 2021; de Medeiros et al., 2020; Marengo et al., 2022). However, some discrepancies among the REMO and RegCM ensembles were detected in areas like Amazonia and southeastern SA when considering ER as one of the extreme events involved in the CE occurrence (for HW + ER.s and DS + ER.s). Heavy rainfall is a complex phenomenon even for the high-resolution modeling, especially in areas like southeastern SA, where the combi-

Figure 9. Projected changes under the Representative Concentration Pathway (RCP) 2.6 and 8.5 scenarios during the late 21st century (2070–2099) for the mean annual frequency of sequential dry-spells and extreme rainfall (DS + ER.s): (a) Maps of changes, expressed as the difference in the number of days compared to the reference period (1981–2010) based on the Coordinated Regional Climate Downscaling Experiment-Coordinated Output for Regional Evaluation regional climate models (RCM) ensemble. Black dots indicate areas where the change signal is robust; (b) Boxplots of the changes for the individual RCMs and their driving earth system models (ESMs), separated according to the seven Intergovernmental Panel on Climate Change regions. Boxes indicate the 25th, 50th, and 75th percentiles and their whiskers show the 5th and 95th percentiles and were created in the native model resolutions. Colors indicate the different ESMs, whereas the ensembles are presented in gray. Light and dark tones indicate the RCP 2.6 and 8.5 scenario (left and right, respectively).

nation of multiple factors at different spatio-temporal scales—such as mesoscale convective activity, frontal systems, the strengthening of the SALLJ and baroclinic instability conditions—strongly modulate the occurrence of these events (Lavín-Gullón et al., 2021; Solman et al., 2021). Furthermore, the Amazon represents the largest tropical rainforest in the world—where land-atmosphere interactions imply essential dynamical components of the climatic system—and precipitation variability is strongly affected by the Andes orographic effect, that interacts with regional atmospheric circulation, evidencing seasonal-to-intraseasonal circulation patterns (Espinoza et al., 2021; Sierra et al., 2021). All these phenomena denote the complex modeling tasks to represent climate extremes over SA, which is critical knowledge to enlighten the future expectations of climate hazards.

In this line, it is worthwhile mentioning that model evaluation is notably dependent on the choice of the reference data set, therefore, caution may be taken when interpreting the RCM biases. Observational uncertainty is a common issue over SA due to the sparseness of meteorological stations and their often-limited temporal coverage, especially in areas like Amazonia and the Andes Mountain range, but also on highly populated regions such as southeastern SA (Condom et al., 2020; Sun et al., 2018). Hence, we explored the differences between ERA5 and the CPC observational data set. Although there were also some discrepancies detected in the frequency and duration of CE, both datasets identified the same areas as hotspots for the occurrence of CE. Note that we used the ERA5 reanalysis as it has the benefit of introducing different observations through the data assimilation process and has a similar spatial resolution to the one presented in the CORDEX-CORE RCMs.

Regarding the future projections of CE, the RCM ensemble usually presented increases in their frequency, especially the ones identified with remarkable frequency and/or duration in specific regions. HW + DS.c are expected to be more frequent in northern SA, northern Chile, and southern Brazil, whereas southeastern SA standed out as the region that showed larger frequencies of DS + ER.s for the late 21st century. Although with some regional differences, these changes are notably strengthened in the worst-case scenario (RCP 8.5), particularly in areas with important metropolitan regions and high-economic development like southeastern SA and eastern Brazil. On one hand, the projected increases in HW + DS over northern and northwestern SA agreed with the observed long-term trends of individual events, indicating an intensification of the extreme warm conditions and a decline in precipitation amounts. Whereas the smaller but still robust changes over southeastern SA followed the detected upward trends in warm extremes. On the other hand, the pattern of changes of sequential DS + ER in the different areas of SA was in accordance with previous findings in the literature, such as a dipole structure in northern SA of increases (decreases) in the dry-days frequency over southern Amazonia (northern Brazil) and the positive (negative) changes over southeastern SA (southern Chile) (Espinoza et al., 2019; Olmo et al., 2020).

Precipitation changes are more variable and season-dependent over southeastern SA, with more heterogeneous changes in dry conditions and increases in ER events that are projected to intensify in the future (Ceron et al., 2020; Regoto et al., 2020; Olmo et al., 2022). This seasonality could have some implications upon the development of agricultural and hydrological practices in the region. In this regard, the RCMs could capture these features of CE on an annual basis, showing that the observed long-term changes are projected to intensify in a context of global warming. Furthermore, this encourages their characterization and the study of their long-term changes seasonally, as differentiated scenarios could be expected.

Although not always robust, the dipole pattern of changes identified in the sequential CE—and especially in DS + ER.s—agreed with the detected increases (decreases) in the dry-days frequency over southern Amazonia (northern Brazil) in the historical period as documented by Espinoza et al. (2019). The authors attributed these long-term changes to modifications in the sea surface temperature and related fluxes over the tropical Atlantic Ocean and in the specific humidity transport, reducing the deep convection in southern Amazonia. Thus, the dry-conditions seemed to be controlling the long-term variability of these sequential CE over northern SA. Additionally, the positive changes over southeastern SA—that were found to be robust even in the RCP 2.6 scenario—were coincident with previous findings on the increasing number of ER events in the region, probably related to modifications in specific atmospheric circulation patterns (Blázquez & Solman, 2020; Olmo et al., 2022). In the same line, a decline in precipitation amounts over central and southern Chile has been detected in the literature working with both observational and model data (Balmaceda-Huarte et al., 2021; Diaz et al., 2020; Olmo et al., 2020), which seems to be influencing the future projections of this CE. These diagnostics evidenced the differentiated influence that the individual extreme events may have on the projected changes of CE throughout the continent. In this way, the RCM ensemble could capture these features, showing that the observed long-term changes are projected to intensify in a context of global warming.

The performance of the ESMs driving the RCM simulations was also explored. The CCS from the ESMs was generally well-conserved by the RCMs, as they tended to present similar change rates but with some differences in specific regions. RegCM often depicted less changes than REMO—like in the case of coincident HW + DS over central and southeastern SA—whereas within the driving ESMs, NorESM1-M—which is considered of low climate sensitivity (Giorgi et al., 2022)—and its corresponding RCMs also tended to show a more reduced pattern of changes. Recall that these high-resolution models mainly inherit this signal from their driving data, although they can introduce some differentiated changes due to their ability to reproduce more sophisticated physical processes (Ambrizzi et al., 2018). Essentially, the RCMs added great spatial detail in their representation of CE in SA—as the Andes Mountain range—and in the evaluation of the long-term expected changes. Hence, although there is some level of model uncertainty, the RCMs provide regional climate information necessary for policy making in terms of CE hotspots and their future projections. Therefore, a larger number of high-resolution climate simulations would be optimal to infer more robust results in a bigger RCM ensemble, helping us to ascertain the future changes in these climate hazards.

Overall, these findings motivate further research to get more insight into the atmospheric processes associated with CE over SA. The climatic drivers behind these CE encompass not only temperature and precipitation—the two surface variables addressed here—but also other variables such as evapotranspiration and atmospheric humidity. In particular, the role of specific humidity and wind at the low-level atmosphere is essential for rainfall variability in different areas of SA, where the SALLJ intraseasonal variability modulates precipitation regimes (Espinoza et al., 2021). Also, it would be interesting to address the influence of teleconnections such as El Niño, which is partially responsible of the variability of climate extremes such as DSs and heavy rainfall (Gulizia & Pirotte, 2021; Iacovone et al., 2020; Reboita et al., 2021), including robust increases detected on dry and warm CE over northern SA (Hao et al., 2018; Wu et al., 2021). Hence, studying their changes under global warming conditions will help us to ascertain the expected changes in CE and the related impacts such as wildfires, water deficit for crops and natural vegetation and human health risk (Bitencourt et al., 2021; Marengo et al., 2022).

Data Availability Statement

The different data sets used in this study are available online. ERA5 reanalysis: https://www.ecmwf.int/en/forecasts/datasets/reanalysis-datasets/era5. CORDEX model outputs: https://esgf-data.dkrz.de/projects/esgf-dkrz/. CPC Global Unified daily gridded dataset observational data set: https://psl.noaa.gov/data/gridded/.

Acknowledgments
The authors acknowledge the Copernicus Climate Change Service for providing the ERA5 reanalysis data set (https://climate.copernicus.eu/climate-reanalysis) and the World Climate Research Program and modeling groups for computing and providing the CMIP5 simulations used as forcing data, as well as the Coordinated Regional Downscaling Experiment (CORDEX) framework and Coordinated Output for Regional Evaluations (CORE). We would like to thank the Earth System Grid Federation for hosting the CORDEX-CORE projections (https://esgf-data.dkrz.de/projects/esgf-dkrz/). We acknowledge the Deutsche Klimarechenzentrum in Hamburg for providing the high-computing capacity. We thank Armelle Remedio for her valuable comments and helpful advice. ME Olmo has been funded by a research grant from the Deutscher Akademischer Austauschdienst (DAAD). ME Olmo and ML Bettolli have been funded by the Argentinian projects 2018-20020170100117BA, 20020170100357BA from the University of Buenos Aires and the ANPCyT PICT-2018-02496 and PICT-2019-02933. Open access funding enabled and organized by Projekt DEAL.

References

Almeira, G., Rusticucci, M., & Suaya, M. (2016). Relación entre mortalidad y temperaturas extremas en Buenos Aires y Rosario. *Meteorológica*, *41*, 65–79.

Ambrizzi, T., Reboita, M. S., Porfirio da Rocha, R., & Llopart, M. (2018). The state-of-the-art and fundamental aspects of regional climate modeling in South America. *Annals of the New York Academy of Sciences*, *1436*(1), 98–120. https://doi.org/10.1111/nyas.13932

Balmaceda-Huarte, R., Olmo, M. E., Bettolli, M. L., & Poggi, M. (2021). Evaluation of multiple reanalyses in reproducing the spatio-temporal variability of temperature and precipitation indices over Southern South America. *International Journal of Climatology*, *41*(12), 5572–5595. https://doi.org/10.1002/joc.7142

Bettolli, M. L., Solman, S., da Rocha, R. P., Llopart, M., Gutiérrez, J. M., Fernández, J., et al. (2021). The CORDEX flagship pilot study in Southeastern South America: A comparative study of statistical and dynamical downscaling mod-els in simulating daily extreme precipitation events. *Climate Dynamics*, *56*(5–6), 1589–1608. https://doi.org/10.1007/s00382-020-05549-z

Bevacqua, E., De Michele, C., Manning, C., Couasnon, A., Ribeiro, A. F. S., Ramos, A. M., et al. (2021). Guidelines for studying diverse types of compound weather and climate events. *Earth's Future*, *9*(11), e2021EF002340. https://doi.org/10.1029/2021EF002340

Bitencourt, D. P., Muniz Alves, L., Shibuya, E. K., de Ângelo da Cunha, I., & Estevam de Souza, J. P. (2021). Climate change impacts on heat stress in Brazil—Past, present, and future implications for occupational heat exposure. *International Journal of Climatology*, *41*(Suppl. 1), E2741–E2756. https://doi.org/10.1002/joc.6877

Blázquez, J., & Solman, S. (2020). Multiscale precipitation variability and extremes over south America: Analysis of future changes from a set of CORDEX regional climate model simulations. *Climate Dynamics*, *55*(7–8), 2089–2106. https://doi.org/10.1007/s00382-020-05370-8

Brouillet, A., & Joussaume, S. (2019). Investigating the role of the relative humidity in the co-occurrence of temperature and heat stress extremes in CMIP5 projections. *Geophysical Research Letters*, *46*(20), 11435–11443. https://doi.org/10.1029/2019GL084156

Carril, A., Cavalcanti, I. F. A., Menéndez, C., Sörensson, A., López de la Franca Arema, N., Rivera, J., et al. (2016). Extreme events in La Plata basin: A retrospective analysis of what we have learned during CLARIS-LPB project. *Climate Research*, *68*(2–3), 95–116. https://doi.org/10.3354/cr01374

Cavalcanti, I., Carril, A., Penalba, O., Grimm, A. M., Menéndez, C., Sanchez, E., et al. (2015). Precipitation extremes over La Plata basin—Review and new results from observations and climate simulations. *Journal of Hydrology*, *523*, 211–230. https://doi.org/10.1016/j.jhydrol.2015.01.028

Cerón, W. L., Kayano, M. T., Andreoli, R. V., Avila-Diaz, A., Ayes, I., Freitas, E. D., et al. (2020). Recent intensification of extreme precipitation events in the La Plata Basin in Southern South America (1981–2018). *Atmospheric Research*, *249*, 105299. https://doi.org/10.1016/j.atmosres.2020.105299

Coelho, C. A. S., De Oliveira, C. P., Ambrizzi, T., Reboita, M. S., Carpenedo, C. B., Campos, J. L., et al. (2016). The 2014 Southeast Brazil austral summer drought: Regional scale mechanisms and teleconnections. *Climate Dynamics*, *46*(11–12), 3737–3752. https://doi.org/10.1007/s00382-015-2800-1

Condom, T., Martínez, R., Pabón, J. D., Costa, F., Pineda, L., Nieto, J. J., et al. (2020). Climatological and hydrological observations for the South American Andes: In situ stations, satellite, and reanalysis data sets. *Frontiers of Earth Science*, *8*, 92. https://doi.org/10.3389/feart.2020.00092

Coppola, E., Raffaele, F., Giorgi, F., Giuliani, G., Xuejie, G., Ciarlo, J. M., et al. (2021). Climate hazard indices projections based on CORDEX-CORE, CMIP5 and CMIP6 ensemble. *Climate Dynamics*, *57*(5), 1293–1383. https://doi.org/10.1007/s00382-021-05640-z

de Medeiros, F. J., de Oliveira, C. P., & Torres, R. R. (2020). Climatic aspects and vertical structure circulation associated with the severe drought in Northeast Brazil (2012–2016). *Climate Dynamics*, *55*(9–10), 2327–2341. https://doi.org/10.1007/s00382-020-05385-1

de Medeiros, F. J., Gomes, R. d. S., Coutinho, M. D. L., & Lima, K. C. (2022). Meteorological droughts and water resources: Historical and future perspectives for Rio Grande do Norte state, Northeast Brazil. *International Journal of Climatology*, 1–20. https://doi.org/10.1002/joc.7624

Dereczynski, C., Chou, S. C., Lyra, A., Sondermann, M., Regoto, P., Tavares, P., et al. (2020). Downscaling of climate extremes over South America–Part I: Model evaluation in the reference climate. *Weather and Climate Extremes*, *29*, 100273. https://doi.org/10.1016/j.wace.2020.100273

Díaz, L. B., Saurral, R. I., & Vera, C. S. (2020). Assessment of South America summer rainfall climatology and trends in a set of global climate models large ensembles. *International Journal of Climatology*, *41*, (S1), 1–19. https://doi.org/10.1002/joc.6643

Di Luca, A., Argüeso, D., Evans, J. P., de Elía, R., & Laprise, R. (2016). Quanti-fying the overall added value of dynamical downscaling and the contribution from different spatial scales. *Journal of Geophysical Research: Atmospheres*, *121*(4), 1575–1590. https://doi.org/10.1002/2015JD024009

Espinoza, J. C., Arias, P. A., Moron, V., Junquas, C., Segura, H., Sierra-Pérez, J., et al. (2021). Recent changes in the atmospheric circulation patterns during the dry-to wet transition season in South tropical South America (1979–2020): Impacts on precipitation and fire season. *Journal of Climate*, *34*, 9025–9042. https://doi.org/10.1175/JCLI-D-21-0303.1

Espinoza, J. C., Garreaud, R., Poveda, G., Arias, P. A., Molina-Carpio, J., Masiokas, M., et al. (2020). Hydroclimate of the Andes part I: Main climatic features. *Frontiers of Earth Science*, *8*, 64. https://doi.org/10.3389/feart.2020.00064

Espinoza, J. C., Ronchail, J., Marengo, J. A., & Segura, H. (2019). Contrasting north-south changes in Amazon wet-day and dry-day frequency and related atmospheric features. *Climate Dynamics*, *116*(9–10), 5413–5430. https://doi.org/10.1007/s00382-018-4462-2

Giorgi, F., Coppola, E., Jacob, D., Teichmann, C., Abba Omar, S., Ashfaq, M., et al. (2022). The CORDEX-CORE EXP-I initiative: Description and highlight results from the initial analysis. *Bulletin of the American Meteorological Society*, *103*(2), E293–E310. https://doi.org/10.1175/BAMS-D-21-0119.1

Giorgi, F., Coppola, E., Solmon, F., Mariotti, L., Sylla, M. B., Bi, X., et al. (2012). RegCM4: Model description and preliminary tests over multiple CORDEX domains. *Climate Research*, *52*, 7–29. https://doi.org/10.3354/cr01018

Gulizia, C., & Pirotte, M. N. (2021). Characterization of simulated extreme El Niño events and projected impacts on South American climate extremes by a set of Coupled Model Intercomparison Project Phase 5 global climate models. *International Journal of Climatology*, *42*, 1–15. https://doi.org/10.1002/joc.7231

Gutowski, J. W., Giorgi, F., Timbal, B., Frigon, A., Jacob, D., Kang, H. S., et al. (2016). WCRP COordinated regional downscaling EXperiment (CORDEX): A diagnostic MIP for CMIP6. *Geoscientific 728 Model Development*, *9*(11), 4087–4095. https://doi.org/10.5194/gmd-9-4087-2016

Hao, Z., Singh, V. P., & Hao, F. (2018). Compound extremes in hydroclimatology: A review. *Water*, *10*(6), 718. https://doi.org/10.3390/w10060718

Hersbach, H., Bell, B., Berrisford, P., Hirahara, S., Horanyi, A., Munoz-Sabater, J., et al. (2020). The ERA5 global reanalysis [Dataset]. Quarterly Journal of the Royal Meteorological Society, *146*(730), 1999–2049. https://doi.org/10.1002/qj.3803

Iacovone, M. F., Pántano, V. C., & Penalba, O. C. (2020). Consecutive dry and wet days over South America and their association with ENSO events, in CMIP5 simulations. *Theoretical and Applied Climatology*, *142*(1–2), 791–804. https://doi.org/10.1007/s00704-020-03324-y

IPCC. (2012). In C. B., Field, V., Barros, T. F., Stocker, D., Qin, D. J., Dokken, (Eds.), *Managing the risks of extreme events and disasters to advance climate change adaptation*. Cambridge University Press.

IPCC. (2021). Climate change 2021: The physical science basis. In V., Masson-Delmotte, P., Zhai, A., Pirani, S. L., Connors, C., Péan, (Eds.), *Contribution of working group I to the sixth assessment report of the intergovernmental panel on climate change Masson-Delmotte*. Cambridge University Press. In press. https://doi.org/10.1017/9781009157896

Iturbide, M., Gutiérrez, J., Alves, L., Bedia, J., Cimadevilla, E., Cofiño, A., et al. (2020). An update of IPCC climate reference regions for subcontinental analysis of climate model data: Definition and aggregated data sets. https://doi.org/10.5194/essd-2019-258

Lavín-Gullón, A., Feijoó, M., Solman, S., Fernández, J., Rocha, R., & Bettolli, M. (2021). Synoptic forcing associated with extreme precipita-tion events over Southeastern South America as depicted by a CORDEX FPS set of convection-permitting RCMs. *Climate Dynamics*, *56*(9–10), 3187–3203. https://doi.org/10.1007/s00382-021-05637-8

Libonati, R., Geirinhas, J. L., Silva, P. S., Russo, A., Rodrigues, J. A., Belem, L. B. C., et al. (2022). Assessing the role of compound droughts and heatwave events on unprecedented 2020 wildfires in the Pantanal. *Environmental Research Letters*, *17*(1), 015005. https://doi.org/10.1088/1748-9326/ac462e

Llopart, M., da Rocha, R. P., Reboita, M., & Cuadra, S. (2017). Sensitivity of simulated South America climate to the land surface schemes in RegCM4. *Climate Dynamics*, *49*(11–12), 3975–3987. https://doi.org/10.1007/s00382-017-3557-5

López-Franca, N., Zaninelli, P. G., Carril, A. F., Menendez, C., & Sanchez, E. (2016). Changes in temperature extremes for 21st century scenarios over South America derived from a multi-model ensemble of regional climate models. *Climate Research*, *68*(2–3), 151–167. https://doi.org/10.3354/cr01393

Marengo, J. A., Ambrizzi, T., Barreto, N., Cunha, A. P., Ramos, A. M., Skansi, M., et al. (2022). The heat wave of October 2020 in central South America. *International Journal of Climatology*, *42*(4), 2281–2298. https://doi.org/10.1002/joc.7365

Marengo, J. A., Camarinha, P. I., Alves, L. M., Diniz, F., & Betts, R. A. (2021). Extreme rainfall and hydro-geo-meteorological disaster risk in 1.5, 2.0, and 4.0°C global warming scenarios: An analysis for Brazil. *Frontiers in Climate*, *3*, 610433. https://doi.org/10.3389/fclim.2021.610433

Moss, R. H., Edmonds, J. A., Hibbard, K. A., Manning, M. R., Rose, S. K., Van Vuuren, D. P., et al. (2010). The next generation of scenarios for climate change research and assessment. *Nature*, *463*(7282), 747–756. https://doi.org/10.1038/nature08823

Olmo, M., Bettolli, M. L., & Rusticucci, M. (2020). Atmospheric circulation influence on temperature and precipitation individual and compound daily extreme events: Spatial variability and trends over Southern South America. *Weather and Climate Extremes*, *29*, 100267. https://doi.org/10.1016/j.wace.2020.100267

Olmo, M. E., Balmaceda-Huarte, R., & Bettolli, M. L. (2022). Multi-model ensemble of statistically downscaled GCMs over Southeastern South America: Historical evaluation and future projections of daily precipitation with focus on extremes. *Climate Dynamics*, *59*(9–10), 3051–3068. https://doi.org/10.1007/s00382-022-06236-x

Olmo, M. E., & Bettolli, M. L. (2021). Extreme daily precipitation in Southern South America: Statistical characterization and circulation types using observational datasets and regional climate models. *Climate Dynamics*, *57*(3–4), 895–916. https://doi.org/10.1007/s00382-021-05748-2

Orth, R., Sungmin, O., Zscheischler, J., Mahecha, M. D., & Reichstein, M. (2021). Contrasting biophysical and societal impacts of hydro-meteorological extremes. *Environmental Research Letters*, *17*(1), 014044. https://doi.org/10.1088/1748-9326/ac4139

Penalba, O. C., & Rivera, J. (2016). Regional aspects of future precipitation and meteorological drought characteristics over Southern South America projected by a CMIP5 multi-model ensemble. *International Journal of Climatology*, *36*(2), 974–986. https://doi.org/10.1002/joc.4398

Rasmussen, K. L., & Houze, R. A. (2016). Convective initiation near the Andes in subtropical South America. *Monthly Weather Review*, *144*, 2351–2374. https://doi.org/10.1175/MWR-D-15-0058.1

Reboita, M., Ambrizzi, S. T., Crespo, N. M., Dutra, L. M. M., Ferreira, G. W. S., Rehbein, D., et al. (2021). Impacts of teleconnection patterns on South America climate: A review. *Annals of the New York Academy of Sciences*, *1504*(1), 116–153. https://doi.org/10.1111/nyas.14592

Reboita, M. S., Fernandez, J. P. R., Pereira Llopart, M., Porfirio da Rocha, R., Albertani Pampuch, L., & Cruz, F. T. (2014). Assessment of RegCM4.3 over the CORDEX South America domain: Sensitivity analysis for physical parameterization schemes. *Climate Research*, *60*(3), 215–234. https://doi.org/10.3354/cr01239

Regoto, P., Dereczynski, C., Chou, S. C., & Bazzanela, A. C. (2020). Observed changes in air temperature and precipitation extremes over Brazil. *International Journal of Climatology*, *41*, (11), 1–18. https://doi.org/10.1002/joc.7119

Remedio, A. R., Teichmann, C., Buntemeyer, L., Sieck, K., Weber, T., Rechid, D., et al. (2019). Evaluation of new CORDEX simulations using an updated Köeppen–Trewartha climate classification. *Atmosphere*, *10*(11), 726. https://doi.org/10.3390/atmos10110726

Ridder, N. N., Pitman, A. J., & Ukkola, A. M. (2021). Do CMIP6 climate models simulate global or regional compound events skillfully? *Geophysical Research Letters*, *48*(2), e2020GL091152. https://doi.org/10.1029/2020GL091152

Salio, P., Nicolini, M., & Zipser, E. J. (2007). Mesoscale convec-tive systems over Southeastern South America and their rela-tionship with the South American low level jet. *Monthly Weather Review*, *135*(4), 1290–1309. https://doi.org/10.1175/MWR3305.1

Sierra, J. P., Junquas, C., Espinoza, J. C., Segura, H., Condom, T., Andrade, M., et al. (2021). Deforestation impacts on Amazon-Andes hydroclimatic connectivity. *Climate Dynamics*, *58*(9–10), 2609–2636. https://doi.org/10.1007/s00382-021-06025-y

Silva Junior, C. H. L., Aragão, L. E. O. C., Anderson, L. O., Fonseca, M. G., Shimabukuro, Y. E., Vancutsem, C., et al. (2020). Persistent collapse of biomass in Amazonian forest edges following deforestation leads to unaccounted carbon losses. *Science Advances*, *6*(40). eaaz8360. https://doi.org/10.1126/sciadv.aaz8360

Solman, S. A., Bettolli, M. L., Doyle, M. E., Olmo, M. E., Feijoo, M., Martínez, D., et al. (2021). Evaluation of multi-ple downscaling tools for simulating extreme precipitation events over Southeastern South America: A case study approach. *Climate Dynamics*, *57*(3–4), 1241–1264. https://doi.org/10.1007/s00382-021-05770-4

Solman, S. A., & Blázquez, J. (2019). Multiscale precipitation variability over South America: Analysis of the added value of CORDEX RCM simulations. *Climate Dynamics*, *53*(3–4), 1547–1565. https://doi.org/10.1007/s00382-019-04689-1

Sun, Q., Miao, C., Duan, Q., Ashouri, H., Sorooshian, S., & Hsu, K.-L. (2018). A review of global precipitation data sets: Data sources, estimation, and inter-comparisons. *Reviews of Geophysics*, *56*(1), 79–107. https://doi.org/10.1002/2017RG000574

Taylor, K. E., Stouffer, R. J., & Meehl, G. A. (2012). An Overview of CMIP5 and the Experiment 908 Design. [Dataset]. Bulletin of the American Meteorological Society, *93*(4), 485–498. Retrieved from 10.1175/BAMS-D-11-00094.1

Teichmann, C., Jacob, D., Remedio, A. R., Remke, T., Buntemeyer, L., Hoffmann, P., et al. (2020). Assessing mean climate change signals in the global CORDEX-CORE ensemble. *Climate Dynamics*. https://doi.org/10.1007/s00382-020-05494-x

Tencer, B., Bettolli, M. L., & Rusticucci, M. (2016). Compound temperature and precipitation extreme events in Southern South America: Associated atmospheric circulation and simulations by a multi-RCM ensemble. *Climate Research*, *68*(2–3), 183–199. https://doi.org/10.3354/cr01396

Tencer, B., Weaver, A., & Zwiers, F. (2014). Joint occurrence of daily temperature and precipitation extreme events over Canada. *Journal of Applied Meteorology and Climatology*, *53*(9), 2148–2162. https://doi.org/10.1175/jamc-d-13-0361.1

Vogel, M. M., Hauser, M., & Seneviratne, S. (2020). Projected changes in hot, dry and wet extreme events' clusters in CMIP6 multi-model ensemble. *Environmental Research Letters*, *15*(9), 094021. https://doi.org/10.1088/1748-9326/ab90a7

Vörösmarty, C. J., de Guenni, L. B., Wollheim, W. M., Pellerin, B., Bjerklie, D., Cardoso, M., et al. (2013). Extreme rainfall, vulnerability and risk: A continental-scale assessment for south America. *Philosophical transactions of the royal society a: mathematical, physical and engineering sciences*, *371*(2002), 20120408. https://doi.org/10.1098/rsta.2012.0408

Weber, T., Bowyer, P., Rechid, D., Pfeifer, S., Raffaele, F., Remedio, A. R., et al. (2020). 929 Analysis of compound climate extremes and exposed population in Africa under two different 930 emission scenarios. *Earth's Future*, *8*, e2019EF001473. https://doi.org/10.1029/2019EF001473

Wu, X., Hao, Z., Tang, Q., Singh, V. P., Zhang, X., & Hao, F. (2021). Projected increase in compound dry and hot events over global land areas. *International Journal of Climatology*, *41*(1), 393–403. https://doi.org/10.1002/joc.6626

Xie, P., Chen, M., Yang, S., Yatagai, A., Hayasaka, T., Fukushima, Y., & Liu, C. (2007). A gauge-based analysis of daily precipitation over East Asia [Dataset]. *Journal of Hydrometeorology*, *8*(3), 607–626. https://doi.org/10.1175/JHM583.1

Zscheischler, J., & Seneviratne, S. (2017). Dependence of drivers affects risks associated with compound events. *Science Advances*, *3*(6), e1700263. https://doi.org/10.1126/sciadv.1700263

Zscheischler, J., Westra, S., Van Den Hurk, B. J., Seneviratne, S. I., Ward, P. J., Pitman, A., et al. (2018). Future climate risk from compound events. *Nature Climate Change*, *8*(6), 469–477. https://doi.org/10.1038/s41558-018-0156-3